Articles

Selective Protein−Protein Interactions Direct Channeling of Intermediates between Polyketide Synthase Modules†

Stuart Y. Tsuji,‡ David E. Cane,§ and Chaitan Khosla*,‡,||,⊥

Departments of Chemical Engineering, Chemistry, and Biochemistry, Stanford University, Stanford, California 94305, and Department of Chemistry, Brown University, Providence, Rhode Island 02912

Received October 24, 2000; Revised Manuscript Received December 22, 2000

ABSTRACT: Polyketide synthases (PKSs) have represented fertile targets for rational manipulation via protein engineering ever since their modular architecture was first recognized. However, the mechanistic principles by which biosynthetic intermediates are sequentially channeled between modules remain poorly understood. Here we demonstrate the importance of complementarity in a remarkably simple, repetitive structural motif within these megasynthases that has been implicated to affect intermodular chain transfer [Gokhale, R. S., et al. (1999) *Science 284*, 482]. The C- and N-terminal ends of adjacent PKS polypeptides are capped by short peptides of 20−40 residues. Mismatched sequences abolish intermodular chain transfer without affecting the activity of individual modules, whereas matched sequences can facilitate the channeling of intermediates between ordinarily nonconsecutive modules. Thus, in addition to substrate−PKS interactions and domain−domain interactions, these short interpolypeptide sequences represent a third determinant of selective chain transfer that must be taken into consideration in the protein engineering of PKSs. Preliminary biophysical studies on synthetic peptide mimics of these linkers suggest that they may adopt coiled-coil conformations.

Modular polyketide synthases (PKSs)[1] are multifunctional enzymes that are organized into multiple catalytic "modules", each comprised of a set of distinct, catalytically functional domains. The core of each module contains a ketosynthase (KS), acyltransferase, and acyl carrier protein (ACP) domain. As illustrated for the deoxyerythronolide B synthase (DEBS) system (Figure 1) (*1*, *2*), these three core domains catalyze the condensation of a single extender unit onto the polyketide intermediate before passing the newly elongated chain to the next module for another round of condensation. (A variable number of postcondensation reactions can be catalyzed within each module, depending on the types of active sites available for such chemistry.) This extension process occurs in an assembly line fashion through the entire sequence of modules. Since PKS modules comprise natural, integrated catalytic units, reorganizing entire modules, rather than individual domains, provides an attractive method for exploiting the combinatorial potential of this biochemistry. Before realizing this strategy, the recognition features of modules need to be defined.

In addition to housing six modules, the three polypeptides of DEBS each possess short, nonconserved segments of amino acid residues located at the N- and C-termini of adjacent polypeptides (shown with complementary symbols in Figure 1). A previous study has emphasized the importance of keeping these interpolypeptide "linkers" intact during the engineering of chimeric PKSs (*3*). To dissect the precise role of these linkers in mediating intermodular interactions, an in vitro system consisting of a donor module and an acceptor module was developed and kinetically characterized. Each of the components of this functional linker pair could then be replaced with counterparts from other naturally occurring linker pairs. The results of these experiments support the emerging understanding that the linker regions outside a module's conserved catalytic domains impact its interactions with other modules. In addition to their importance in functionally connecting modules, these short sequences also play an active role in the protein−protein recognition of modules, helping to maintain the selective transfer of intermediates.

MATERIALS AND METHODS

Reagents and Chemicals. DL-[2-*methyl*-^{14}C]Methylmalonyl-CoA (56.4 mCi/mmol) was obtained from ARC, Inc.

† This research was supported by grants from the National Institutes of Health (CA66736 to C.K. and GM22172 to D.E.C.). S.Y.T. is a recipient of a National Science Foundation Predoctoral Fellowship.

* Address correspondence to this author. Phone/Fax: 650-723-6538. E-mail: ck@chemeng.stanford.edu.

‡ Department of Chemical Engineering, Stanford University.

§ Department of Chemistry, Brown University.

|| Department of Chemistry, Stanford University.

⊥ Department of Biochemistry, Stanford University.

[1] Abbreviations: PKS, polyketide synthase; KS, ketosynthase; ACP, acyl carrier protein; DEBS, 6-deoxyerythronolide B synthase; M2, module 2 of DEBS; M2(4), module 2 with C-terminal linker from module 4; M3 + TE, module 3 fused to thioesterase; (5)M3 + TE, module 3 with N-terminal linker from module 5; M2−M3, complex of module 2 and module 3; NDK, (2*S*,3*R*)-2-methyl-3-hydroxypentanoic acid diketide.

10.1021/bi002463n CCC: $20.00
Published on Web 02/02/2001

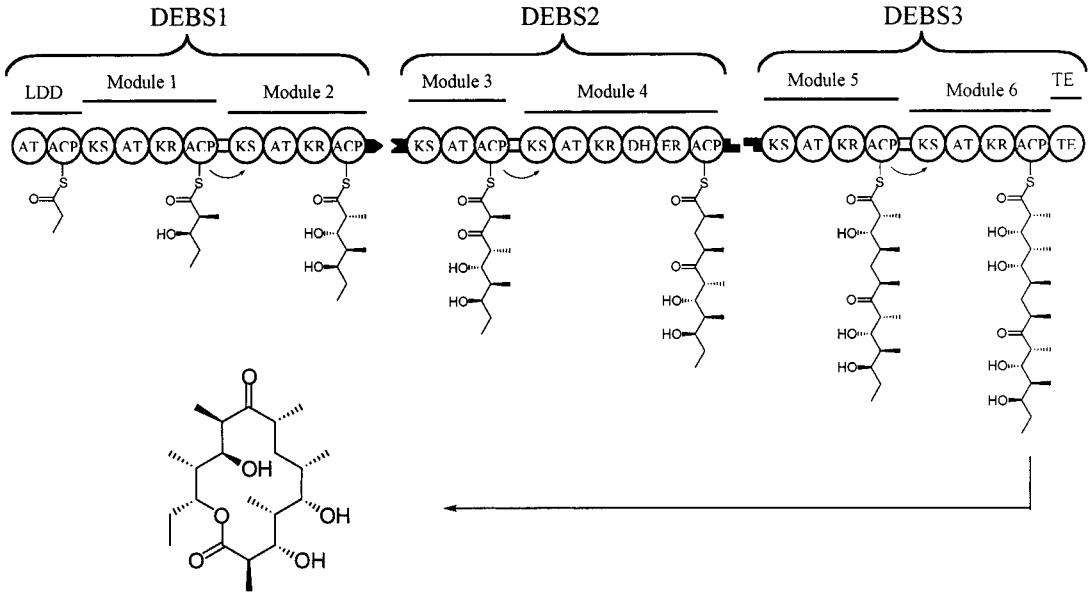

FIGURE 1: Schematic diagram of the biosynthesis of 6-dEB by 6-deoxyerythronolide B synthase. Each polypeptide, DEBS1, DEBS2, and DEBS3, contains two modules, and each module comprises a set of active site domains responsible for addition and modification of an extender unit. The short "linker" regions are located at the N- and C-termini; their shapes exemplify the complementarity demonstrated by each pair.

The N-terminal linker of M3 was synthesized by New England Peptide (Fitchburg, MA). The peptide sequence was as follows. M3 N-term: H_2N-MTDSEKVAEYLRRATLD-LRAARQRIRELESD-amide.

Construction of Plasmids. Plasmid pBP19 contains module 2 of DEBS (M2) and is a derivative of pRSG64 (*3*), where the thioesterase domain was replaced with a *Spe*I−*Eco*RI fragment containing the natural C-terminal linker for module 2 to make pBP19. Plasmid pST179 encodes a derivative of M2 containing the C-terminal linker of DEBS module 4 (M4). The C-terminal linker of M4 was obtained as a *Spe*I−*Eco*RI fragment by PCR using the primers 5′-ACT AGT **AGG CTG TTC GCG GCC TCA C**-3′ and 5′-G GGA ATT **CAG GTC CTC TCC CCC GC**-3′ (bold sequences complement DEBS sequence). The PCR amplicon was inserted after M2 using the engineered sites, yielding pST179. This plasmid, pRSG34, encodes module 3 of DEBS (M3) with its own N-terminal linker and with the thioesterase fused to the C-terminus. Its construction has been described previously (*3*). Plasmid pST132 encodes a derivative of M3 + TE, where the natural N-terminal linker of pRSG34 has been replaced with the N-terminal linker of module 5 of DEBS (M5). This substitution required the replacement of the *Nde*I−*Bsa*BI fragment of pRSG34 with the corresponding fragment from pJRJ10 (*6*). All constructs were cloned into pET-21c (Novagen) vectors for expression in *Escherichia coli*.

Strain and Culture Conditions. Expression of the desired proteins was achieved by transforming the above plasmids into an engineered strain of *E. coli* BL21(DE3) containing the *sfp* phosphopantetheinyl transferase gene from *Bacillus subtilis* (*7*). The *sfp* gene product was required to posttranslationally modify the acyl carrier protein (ACP) domains by phoshopantetheinylating the apo-ACP (*3*). Cells containing the expression plasmids were selected with carbenicillin and used to inoculate a 10−20 mL LB medium starter culture grown at 37 °C. After 6 h, the cells were pelleted and used to inoculate two 2 L flasks containing 1 L of LB medium each. The flasks were shaken at 250 rpm at 37 °C until the culture optical density at 600 nm (OD_{600}) was 0.6. The flasks were placed in a water bath to cool the cells to 22 °C (ca. 10 min) and then induced with 0.5 mM isopropyl β-D-thiogalactopyranoside at an $OD_{600} = 0.8$. Flasks were then stirred at 22−24 °C for 10−14 h.

Purification of Proteins. After induction, the cells were harvested via centrifugation and washed in 50 mM Tris (pH 8) and 1 mM ethylenediaminetetraacetic acid (EDTA) before being resuspended in disruption buffer [200 mM sodium chloride, 200 mM sodium phosphate, 2.5 mM dithiothreitol (DTT), 2.5 mM EDTA, 1.5 mM benzamidine, pepstatin and leupeptin (2 mg/L), and 30% (w/v) glycerol]. The cell suspension was lysed at 1250 psi using a French press and then centrifuged. Polyethylenimine was added to the supernatant to 0.15% to precipitate nucleic acids. Following the centrifugation (20 min at 33300*g*) to remove the nucleic acids, ammonium sulfate was added to the supernatant until a 50% (w/v) saturation was achieved and allowed to precipitate for 2−3 h. The pellet following a 45 min centrifugation (33300*g*) was resuspended in buffer A [100 mM sodium phosphate (pH 7.2), 2 mM DTT, 1 mM EDTA, and 20% (v/v) glycerol]. The resulting suspension was applied in 2.5 mL aliquots to a 9.1 mL gel filtration column (PD-10, Pharmacia) equilibrated with buffer B (buffer A + 1 M ammonium sulfate) and eluted in 3.5 mL of buffer B. This eluant was applied to a 30 mL hydrophobic-interaction column (Butyl-Sepharose 4 FastFlow, Pharmacia) at 1 mL/min. Elution was performed at 1 mL/min with stepwise changes in buffer starting from 100% buffer B, to 40%, 20%, and 0%. Steps were made when the absorbance at 280 nm approached baseline. Fractions were 10 mL, and those containing the protein of interest (typically eluted with 0% buffer B) were pooled and applied to an anion-exchange column (Resource Q, 6 mL, Pharmacia) at 1 mL/min. A gradient of 0−0.15 M NaCl in buffer A was run at 1 mL/min for 3 column volumes, followed by a gentle gradient of 0.15−0.30 M NaCl at 1 mL/min for 10 column volumes.

Fractions of 2 mL were collected, and those containing concentrated protein (typically 0.22−0.25 M NaCl) were pooled and further concentrated on Centriprep 50 membranes (50 kDa molecular mass cutoff; Amicon) to a concentration of 0.1−4 mg/mL. Protein concentrations were measured via the modified Lowry assay (Sigma) and densitometric analysis of SDS−PAGE gels stained with Coomassie Blue. On the basis of the densitometry data, all proteins were determined to be >90% pure.

In Vitro Polyketide Production. Assays of individual modules contained 1.0 μM protein, 1−10 mM *N*-acetylcysteamine thioester of the "natural" (2*S*,3*R*)-2-methyl-3-hydroxypentanoic acid diketide (NDK) (**1**), 4 mM NADPH, 440 mM sodium phosphate, 1 mM EDTA, 2.5 mM dithiothreitol (DTT), and 20% w/v glycerol, pH 7.2, in 80 μL. Reactions with M2 or M2(4) included 0.3 mM [^{14}C]-methylmalonyl-CoA (specific activity adjusted to 10.4 mCi/mmol), and those with M3 + TE or (5)M3 + TE included 0.5 mM [^{14}C]methylmalonyl-CoA (specific activity reduced to 1.1 mCi/mmol). [M2(4) refers to a derivative of M2 in which the C-terminal linker has been replaced with its counterpart from module 4, whereas (5)M3 refers to a derivative of M3 in which the N-terminal linker has been replaced with its counterpart from module 5 (see Figure 1).] Both concentrations of methylmalonyl-CoA were saturating, but different concentrations were needed due to the disparate rates of turnover between the modules with and without the thioesterase. The reaction mixtures were preincubated to 30 °C and started with the addition of the methylmalonyl-CoA. The reactions were incubated at 30 °C, and at three to four time points, 20 μL aliquots were removed and quenched with ethyl acetate, which was extracted twice (450 μL total) to isolate the polyketide products. The ethyl acetate layers were pooled, dried in vacuo, and applied to an analytical thin-layer chromatography (TLC) plate (Si250F; Baker). The TLC plate was developed using 50% ethyl acetate in hexanes as the mobile phase (triketide ketolactone **4**, $R_f = 0.5$; triketide lactone **3**, $R_f = 0.4$) and then visualized by electronic autoradiography (InstantImager, Packard Instruments). Product formation was quantified by comparison with standards of the labeled methylmalonyl-CoA. The identity of products **2**, **3**, and **4** has been unambiguously established in earlier in vitro enzymatic studies (*8*, *9*) and was reconfirmed by chromatographic comparison with authentic reference samples.

Assays of M2 and M3 + TE contained 1.0 μM M2 and 0.4−4 μM M3 + TE, 7 mM NDK, 0.5 mM [^{14}C]methylmalonyl-CoA (specific activity reduced to 3.4 mCi/mmol), 4 mM NADPH, 440 mM sodium phosphate, 1 mM EDTA, 2.5 mM DTT, and 20% w/v glycerol, pH 7.2, in 70 μL. Assays of M2(4) and (5)M3 + TE were identical, except they contained 0.5 μM M2(4), 0.5−5 μM (5)M3 + TE, and 0.4 mM [^{14}C]methylmalonyl-CoA (specific activity reduced to 6.2 mCi/mmol). The concentration of M2(4) was limiting in order to facilitate its saturation with (5)M3 + TE. The reactions were prewarmed at 30 °C and initiated by the addition of the methylmalonyl-CoA. As described above, 20 μL aliquots were removed at various time points and processed. Extracts loaded onto TLC plates were separated using either 80% ethyl acetate in hexanes or 5% methanol in dichloromethane, both of which allowed identification of the tetraketide lactone **2** and the triketide lactones **3** and **4**.

Inhibition of Tetraketide Production. The ability of the synthetic peptide to inhibit the transfer reaction, and thus the production of tetraketide, was tested under the same reaction conditions described for the two module coincubations. The concentrations of M2 and M3 + TE were both 1.0 μM, and the concentrations of M2(4) and (5)M3 + TE were 0.5 and 1.0 μM, respectively. The only difference was the addition of the peptide at concentrations ranging from 1 to 100 μM to the assay containing M2 and M3 + TE [or alternatively M2(4) and (5)M3 + TE]. For greater accuracy, each inhibition assay was performed side by side with a control lacking inhibitor. The effect of the inhibitor was thus determined by dividing the inhibited rate by the control rate.

Kinetic Analysis. For individual modules, the steady-state turnover number was determined from the time course of triketide formation, normalized to the concentration of protein. The dependence of the rate on substrate concentration was measured by varying the concentration of NDK while maintaining saturating levels of NADPH and methylmalonyl-CoA. From these data, the k_{cat} and K_M were calculated by fitting the normalized v versus [S] plots to the Michaelis−Menten equation.

For tetraketide formation, the rate of production of tetraketide was recorded for varying concentrations of M3 + TE [or (5)M3 + TE] at a fixed concentration of M2 [or M2(4)] and saturating concentrations of substrates. By fitting the rate dependence of tetraketide to a saturation curve, the maximal velocity (v_{max}) of tetraketide production was determined and was assumed to represent the case where every M2 homodimer was productively associated with an M3 + TE homodimer. Thus, the affinity of this protein−protein interaction could be calculated from the rate of tetraketide formation, as represented in eq 1 ([M2], [M3],

$$v = k_{cat}[\mathrm{M2{-}M3}] \tag{1}$$

and [M2−M3] refer to the concentrations of M2, unbound M3 + TE, and the M2/M3 + TE complex, respectively). Since [M2−M3] is related to the K_D of M2 and M3 + TE as shown in the equation

$$K_D = \frac{[\mathrm{M2}][\mathrm{M3}]}{[\mathrm{M2{-}M3}]} \tag{2}$$

which can be rearranged to yield the equation

$$[\mathrm{M2{-}M3}] = \frac{[\mathrm{M2}]_0[\mathrm{M3}]}{K_D + [\mathrm{M3}]} \tag{3}$$

where $[M2]_0$ = total concentration of M2, the velocity of tetraketide production can be defined relative to the K_D:

$$v = \frac{v_{max}[\mathrm{M3}]}{K_D + [\mathrm{M3}]} \tag{4}$$

where $v = k_{cat}[\mathrm{M2{-}M3}]$ and $v_{max} = k_{cat}[\mathrm{M2}]_0$. Thus, fitting of the v versus [M3] plot (which is equivalent to the bound M3 + TE versus free M3 + TE plot used for Scatchard analysis) to eq 4 allowed determination of the K_D for M2 and M3 + TE association.

CD Spectroscopy. The CD spectrum of the M3 N-terminal peptide was recorded in a 1-mm path-length cell at a sample

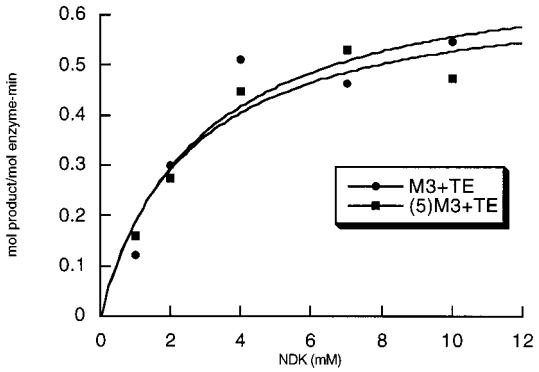

FIGURE 2: Velocity vs [NDK] plot showing the fit of the Michaelis−Menten equation for M3 + TE and (5)M3 + TE alone. The nearly identical k_{cat} values of 0.71 and 0.68 min^{-1} and K_M values of 2.8 and 2.5 μM demonstrate the interchangeability of the linkers for individual modules.

concentration of 100 μM in phosphate-buffered saline (PBS; 0.15 M KCl, 25 mM phosphate, pH 6.9). Measurements were made using an Aviv 62DS spectropolarimeter. Concentration was determined by tyrosine absorbance at 275 nm in 8 M guanidine hydrochloride.

RESULTS

Kinetic Analysis of Individual Modules. To directly measure the effect of linker replacement, individual modules with substituted linkers were kinetically characterized using the natural diketide (NDK) as substrate. The only difference between the M3 + TE and (5)M3 + TE proteins was that the former contained the N-terminal linker of M3, whereas the latter contained the N-terminal linker of M5. As shown in Figure 2, the modules displayed very similar kinetics. The calculated k_{cat} values were 0.71 ± 0.1 and 0.68 ± 0.1 min^{-1} and the K_M values were 2.8 ± 1.5 and 2.5 ± 1.0 μM for M3 + TE and (5)M3 + TE, respectively. Similar experiments were performed to compare M2 and M2(4), where the C-terminal linker of M2 had been swapped. Since the rate of turnover of NDK to triketide lactone **3** by module 2 lacking the fused thioesterase domain was low, however, only an approximate k_{cat} could be estimated [0.02 and 0.03 min^{-1} for M2 and M2(4), respectively]. Thus, replacement of either the N-terminal or the C-terminal linker of a module does not appear to affect its intrinsic catalytic properties.

Kinetic Analysis of M2−M3 Coincubations. Upon coincubation of M2 and M3 + TE in the presence of NDK, methylmalonyl-CoA, and NADPH, tetraketide lactone **2** was formed (Figure 3) with a maximum rate constant of 0.27 ± 0.01 min^{-1}. The k_{cat} of M2 with M3 + TE was determined from the saturation curve determined using a fixed concentration of M2 and a variable concentration of M3 + TE and correlated well with an earlier measurement of 0.23 min^{-1} for formation of the same tetraketide by DEBS1 and M3 + TE (*9*). Thus, the M2 protein described here appears to be a viable alternative to DEBS1 as a donor of the triketide intermediate to M3 + TE. From the saturation curve, a K_D of 1.1 ± 0.1 μM for the M2−M3 + TE interaction could be estimated (Figure 4A; see also Materials and Methods section). Again, this value compares well with the previously reported value of 2.6 μM for DEBS1 and M3 + TE (*10*).

Analogous to the above study, coincubation of M2(4) with (5)M3 + TE allowed examination of the effects of the

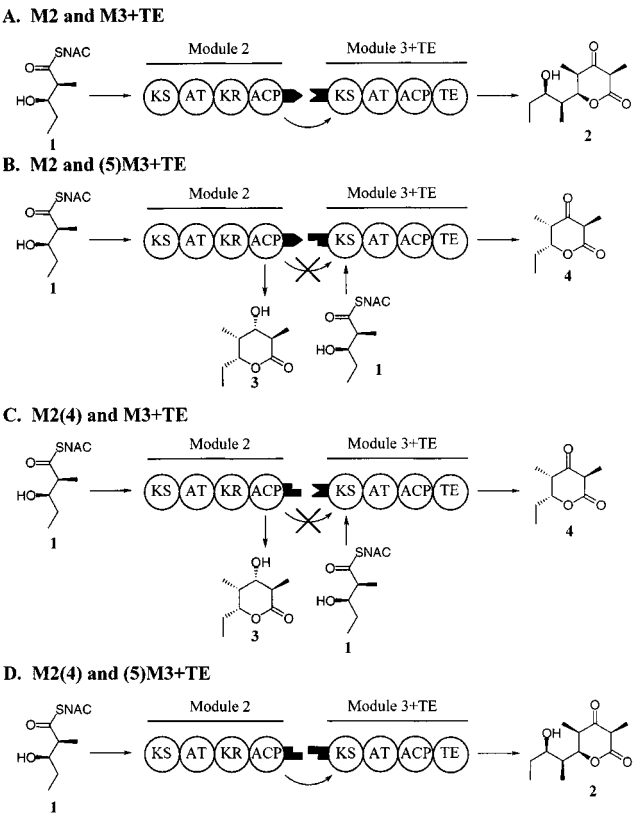

FIGURE 3: Schematic diagram of the interpolypeptide transfer with matched and mismatched linker pairs: (A) wild-type linker pair, M2 C-terminus + M3 N-terminus; (B) mismatched pair, M2 C-terminus + M5 N-terminus; (C) mismatched pair, M4 C-terminus + M3 N-terminus; (D) matched pair, M4 C-terminus + M5 N-terminus.

transplanted DEBS2−DEBS3 linker pair (Figure 1) on chain transfer between modules 2 and 3. The efficiency of chain transfer in the presence of this alternative linker pair (Figure 3D) was established by measuring the same parameters associated with synthesis of the tetraketide lactone **2** [k_{cat} of 0.74 ± 0.06 min^{-1} and a K_D of 2.1 ± 0.4 μM (Figure 4B)].

Effects of Mismatched Linker Pairs. In contrast to the above studies with M2 and M3 + TE (Figure 3A) or M2(4) and (5)M3 + TE (Figure 3D), both of the noncomplementary coincubations [M2 with (5)M3 + TE (Figure 3B) and M2-(4) with M3 + TE (Figure 3C)] produced the tetraketide lactone **2** at severely compromised rates. The highest rate constants that could be measured with either mismatched system were in the range of 0.02−0.03 min^{-1}. Given these low rate constants, the dependence of rate on protein concentration could not be measured. As might be expected, the rate of production of ketolactone **4** increased markedly in both cases relative to the matched incubations above (data not shown), since module 3 remained active in these mismatched coincubations.

Inhibition of Tetraketide Production by a Synthetic Peptide. Sequence analysis using the CoilScan program (*4*, *5*) revealed that the N- and C-terminal interpolypeptide linkers of DEBS contained 15−20 residue segments with strong propensity to assume a coiled-coil structure. Since the N-terminal linker of module 3 is relatively short (31 residues), a peptide corresponding to this sequence was synthesized (see Materials and Methods). As shown in Figure 5, this linker could inhibit the formation of **2** in the presence

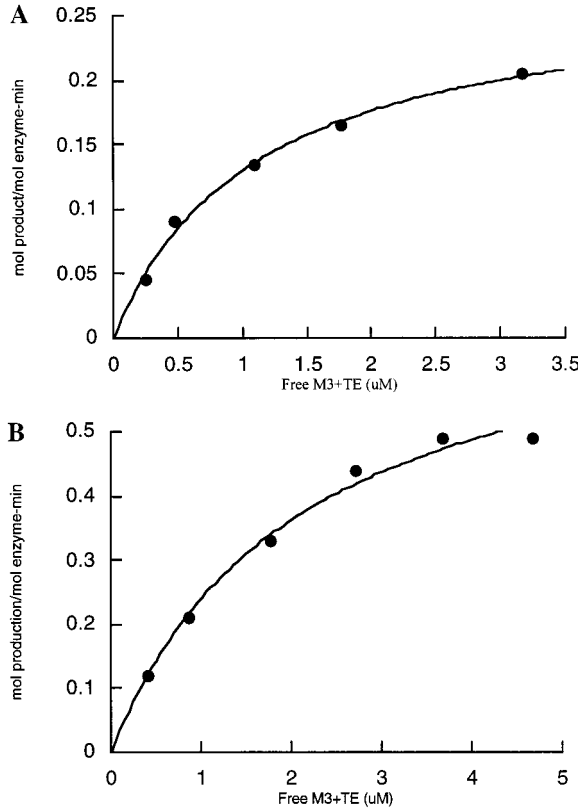

FIGURE 4: Saturation curves of (A) M2 with M3 + TE and (B) M2(4) with (5)M3 + TE showing the effect of increasing M3 concentration on the overall rate of turnover. From these plots, the saturating rates of 0.27 and 0.74 min^{-1} were determined, as were the K_D values of 1.1 and 2.1 μM.

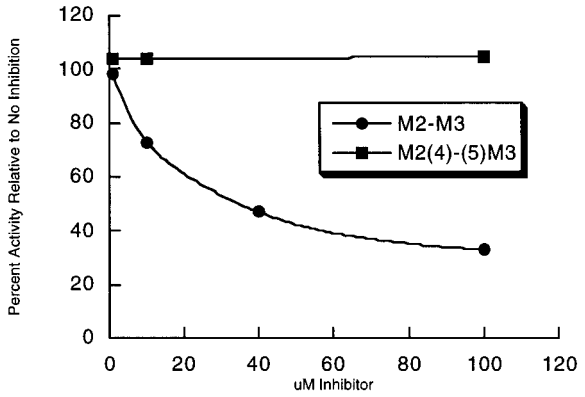

FIGURE 5: Selective inhibition by the synthetic peptide mimic of the N-terminal linker of M3. The linker lowered the overall rate of tetraketide production in a dose-dependent fashion for the transfer using the M2−M3 linker pair. However, it demonstrated no such effect when tetraketide production depended upon interpolypeptide transfer using the M4−M5 linker pair.

of M2 and M3 + TE in a concentration-dependent manner. To test the specificity of this peptide inhibitor, a similar assay was also conducted in the presence of M2(4) and (5)M3 + TE. No inhibitory effect was observed at peptide concentrations up to 100 μM (Figure 5). Furthermore, the peptide also showed no inhibitory effect upon individually assayed modules, including M3 + TE. Thus, isolated peptide linkers appear to be selectively capable of competing for their cognate module-bound partners without affecting their individual catalytic activities.

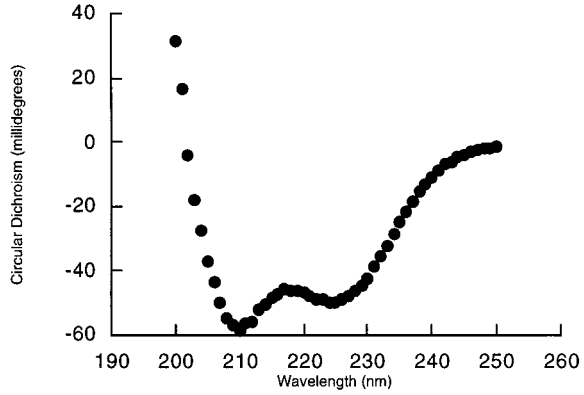

FIGURE 6: The CD spectrum of the peptide mimic shows the minima at 208 and 222 nm indicative of α-helical character. Though only ca. 50% helical, its structural features correlate with the expected coiled-coil motif. Furthermore, its ability to selectively inhibit interpolypeptide transfer verified some recognition ability of the mimic.

The N-terminal linker peptide of M3 was analyzed via circular dichroism (CD) to assess its α-helical character. As shown in Figure 6, the spectrum shows the 208 and 222 nm absorbances characteristic of α-helices. The magnitude of these peaks allowed us to estimate that the peptide was approximately 50% helical (*11*). The CD of the peptide appeared invariant with peptide concentration, salt concentration, and phosphate concentration.

DISCUSSION

Earlier studies suggested the role of structurally intact intermodular linkers in facilitating chain transfer between noncovalently associated modules of PKSs (*3*). Here we have extended and elaborated these findings in several significant ways. First, our results have vividly demonstrated the selectivity associated with linker-mediated chain transfer (Figure 3). Although intermodular chain transfer can occur between modules possessing mismatched linker pairs, a serious kinetic penalty is paid. In contrast, heterologous matched linker pairs can facilitate chain transfer between modules as efficiently as natural pairs. Second, the selectivity associated with linker pair interactions suggests that they might play a key role in the transient assembly of functionally paired complexes of the three DEBS proteins (*12*, *13*). In support of this hypothesis, we have demonstrated that a peptide mimic of the N-terminal linker of DEBS2 can inhibit chain transfer mediated by the linker pair at the DEBS1−DEBS2 interface but not by the linker pair at the DEBS2−DEBS3 interface (Figure 5). Third, we show that the N-terminal linker peptide of DEBS2 has significant (ca. 50%) helical content (Figure 6). This observation is consistent with secondary structure analyses of individual linker sequences, which previously indicated a propensity of these sequences to assume coiled-coil conformations.[2] It should be emphasized that, in order for a coiled-coil motif to facilitate noncovalent docking of two modules, the heterodimer (or heterooligomer) formed by associations between the C-

[2] Note, however, that the proposed implications of the putative coiled coils are different. Whereas Leadlay and co-workers (*19*) have proposed that these terminal coiled coils might stabilize the homodimeric structure of modules, our own proposal (*20*) is that they somehow facilitate intermodular chain transfer.

terminal linker and N-terminal linker must be thermodynamically more favorable than either homodimer. Although the data shown in Figure 6 show helical content of a linker, it does not provide evidence for formation of a coiled-coil structure. Thus, direct evidence for the existence of coiled coils at intermodular interfaces, as well as their implications for selective chain transfer, remains to be obtained.

Earlier studies have demonstrated the importance of two additional molecular recognition events in controlling the overall programming and specificity of PKSs. First, individual modules can discriminate among alternative incoming substrates (*14*); this selectivity appears to reside within the individual ketosynthase domains (*15*, *16*). Second, ketosynthase and ACP domains appear to have some degree of mutual recognition (*17*, *18*). Both of these recognition properties are localized within highly conserved and catalytically critical parts of the large PKS modules. Here we define and dissect a third element of selectivity. In contrast to the previously recognized factors influencing molecular recognition by PKS components, linker-mediated intermodular interactions have been localized to short, nonconserved regions that lie outside the core modules and have no influence on the intrinsic chemistry of the individual modules. Whereas the relative importance of these different factors in controlling the effective vectorial channeling of highly labile polyketide intermediates remains to be established, the remarkable simplicity and modularity of interpolypeptide linkers should provide the protein engineer with a powerful tool to combinatorially manipulate PKS modules for the generation of novel polyketide natural products.

REFERENCES

1. Cortes, J., Haydock, S. F., Roberts, G. A., Bevitt, D. J., and Leadlay, P. F. (1990) *Nature 348*, 176−178.
2. Donadio, S., Staver, M. J., McAlpine, J. B., Swanson, S. J., and Katz, L. (1991) *Science 252*, 675−679.
3. Gokhale, R. S., Tsuji, S. Y., Cane, D. E., and Khosla, C. (1999) *Science 284*, 482−485.
4. Lupas, A., Van Dyke, M., and Stock, J. (1991) *Science 252*, 1162−1164.
5. Lupas, A. (1996) *Methods Enzymol. 266*, 513−525.
6. Jacobsen, J. R., Cane, D. E., and Khosla, C. (1998) *Biochemistry 37*, 4928−4934.
7. Lambalot, R. H., Gehring, A. M., Flugel, R. S., Zuber, P., LaCelle, M., Marahiel, M. A., Reid, R., Khosla, C., and Walsh, C. T. (1996) *Chem. Biol. 3*, 923−936.
8. Pieper, R., Luo, G., Cane, D. E., and Khosla, C. (1995) *J. Am. Chem. Soc. 117*, 11373−11374.
9. Pieper, R., Gokhale, R. S., Luo, G., Cane, D. E., and Khosla, C. (1997) *Biochemistry 36*, 1846−1851.
10. Gokhale, R. S., Hunziker, D., Cane, D. E., and Khosla, C. (1999) *Chem. Biol. 6*, 117−125.
11. Chen, Y. H., Yang, J. T., and Chau, K. H. (1974) *Biochemistry 13*, 3350−3359.
12. Aparicio, J. F., Caffrey, P., Marsden, A. F., Staunton, J., and Leadlay, P. F. (1994) *J. Biol. Chem. 269*, 8524−8528.
13. Pieper, R., Luo, G., Cane, D. E., and Khosla, C. (1995) *Nature 378*, 263−266.
14. Wu, N., Kudo, F., Cane, D. E., and Khosla, C. (2000) *J. Am. Chem. Soc. 122*, 4847−4852.
15. Jacobsen, J. R., Hutchinson, C. R., Cane, D. E., and Khosla, C. (1997) *Science 277*, 367−369.
16. Chuck, J., McPherson, M., Huang, H., Jacobsen, J. R., Khosla, C., and Cane, D. E. (1997) *Chem. Biol. 4*, 757−766.
17. Dreier, J., Shah, A. N., and Khosla, C. (1999) *J. Biol. Chem. 274*, 25108−25112.
18. Ranganathan, A., Timoney, M., Bycroft, M., Cortes, J., Thomas, I. P., Wilkinson, B., Kellenberger, L., Hanefeld, U., Galloway, I. S., Staunton, J., and Leadlay, P. F. (1999) *Chem. Biol. 6*, 731−741.
19. Aparicio, J. F., Molnar, I., Schwecke, T., Konig, A., Haydock, S. F., Khaw, L. E., Staunton, J., and Leadlay, P. F. (1996) *Gene 169*, 9−16.
20. Gokhale, R. S., and Khosla, C. (2000) *Curr. Opin. Chem. Biol. 4*, 22−27.

BI002463N